PERGAMON

Oral Oncology 36 (2000) 286–293

ORAL ONCOLOGY

www.elsevier.com/locate/oraloncology

Classification of clinical autofluorescence spectra of oral leukoplakia using an artificial neural network: a pilot study

H.J. van Staveren [a], R.L.P. van Veen [a], O.C. Speelman [a], M.J.H. Witjes [b], W.M. Star [a,*], J.L.N. Roodenburg [b]

[a] *Department of Clinical Physics, PDT Laboratory, Daniel den Hoed Cancer Center, University Hospital Rotterdam, PO Box 5201, NL-3008 AE Rotterdam, Netherlands*

[b] *Department of Oral and Maxillofacial Surgery and Special Dental Care, University Hospital Groningen, PO Box 30001, NL-9700 RB Groningen, Netherlands*

Received 23 July 1999; accepted 30 August 1999

Abstract

The performance of an artificial neural network was evaluated as an alternative classification technique of autofluorescence spectra of oral leukoplakia, which may reflect the grade of tissue dysplasia. Twenty-two visible lesions of 21 patients suffering from oral leukoplakia and six locations on normal oral mucosa of volunteers were investigated with autofluorescence spectroscopy (420 nm excitation, 465–650 nm emission). Pre-scaled spectra were combined with the corresponding visual and histopathological classifications in order to train artificial neural networks. A trained network is mapping input spectra to tissue characteristics, which was evaluated using a blind set of spectra. Abnormal tissue could be distinguished from normal tissue by a neural network with a sensitivity of 86% and a specificity of 100%. Also, classifying either homogenous or non-homogenous tissue performed reasonably well. Weak or no correlation existed between spectral patterns and verrucous or erosive tissue or the grade of dysplasia, hyperplasia and hyperkeratosis.

Keywords: Artificial neural network; Autofluorescence; Fluorescence spectroscopy; Leukoplakia; Oral mucosa

1. Introduction

There is much clinical interest in the early detection of pre-malignant lesions and malignant tumours, as it can reduce patient morbidity and mortality. Oral leukoplakia is a predominantly white lesion of the oral mucosa that cannot be characterised as any other definable lesion; and some oral leukoplakia will transform into cancer [1]. Patients suffering from (pre)malignant lesions of the oral cavity often have multiple areas of dysplastic mucosa, of which a certain amount is not observed by visual inspection. This condition is referred to as condemned mucosa or field cancerisation. Due to their condemned mucosa, 10–28% of the patients diagnosed with a squamous cell carcinoma (SCC) will develop a second primary tumour within 10 years leading to a poor prognosis. Early detection of field cancerisation of the oral mucosa is essential for a curative treatment and especially patients at risk for developing a second primary tumour may benefit.

Optical spectroscopy of tissue autofluorescence is a sensitive, non-invasive and easily applicable tool for the detection of alterations in the structural and chemical composition of the cells, which may indicate the presence of diseased tissue [2]. Several investigators have reported promising results for autofluorescence spectroscopy on tissues of the upper aerodigestive tract [3–7]. However, the success of diagnosing diseased tissue in a clinical setting will largely depend on the correct correlation of spectra with the grade of tissue dysplasia. An appropriate pattern-recognition algorithm is of crucial importance in the decision of whether an investigated site is considered normal or abnormal. The use of artificial neural networks for pattern recognition has been widely investigated for various medical applications, e.g. electroencephalography [8], ultrasound [9], nuclear magnetic resonance [10], reflectance spectroscopy [11], infrared spectroscopy [12] and autofluorescence spectroscopy

* Corresponding author. Tel.: +31-10-439-11-31; fax: +31-10-439-10-12.

E-mail address: star@kfih.azr.nl (W.M. Star).

1368-8375/00/$ - see front matter
PII: S1368-8375(00)00004-X

[13]. Neural networks often produced results comparable to or better than conventional mathematical analysis, e.g. principal component analysis, multivariate linear regression and *K*-nearest neighbours analysis. These artificial neural networks thus offer a trainable classification technique for autofluorescence spectra that may outperform the conventional spectral analysis.

In this pilot study, patients suffering from visible oral leukoplakia and volunteers with normal oral mucosa have been investigated with autofluorescence spectroscopy. These measurements were combined with visual and histological classifications in order to train and evaluate artificial neural networks.

2. Patients and methods

2.1. Patient population

The autofluorescence spectroscopy study comprised a group of 21 Caucasian patients with 22 visible leukoplakias in the oral cavity, 11 men and 10 women with a mean age of 61 (range 30–81) years, which were included from July 1997 to October 1998 after giving their informed consent (Table 1). Spectral measurements on a lesion in the oral cavity were performed within 10 min, prior to the removal of the leukoplakia by CO_2-laser evaporation. The nature of the leukoplakia had been established 2–3 months earlier by visual inspection and histological examination, for which the necessary biopsy of about 4–8 mm in diameter had been performed at the border of the lesion. Autofluorescence spectra were only taken from lesions with histologically proven leukoplakia.

In addition, autofluorescence spectra of normal oral mucosa were obtained from two investigators at six different locations in the oral cavity; at the left and right side of the cheek, at the left and right side of the floor of the mouth and at the left and right side of the lateral border of the tongue.

2.2. Clinical diagnosis and histology

A lesion was visually classified as homogenous or non-homogenous, where the latter was sub classified as white/verrucous or white/red/erosive. Tissue biopsies were fixed in formaline, sectioned and stained with haematoxylin and eosin for conventional light microscopy. The samples were graded according to established criteria as grade 0–3 dysplasia (no, mild, moderate and severe), grade 0–2 hyperplasia (no, moderate and severe) and grade 0–2 hyperkeratosis (no, moderate and severe) by a pathologist, blinded for any other classifications.

2.3. Autofluorescence spectroscopy

The set-up (Fig. 1a) consisted of a Xe-lamp with monochromator (Photomax 60100 + 77250, Oriel Instruments Corporation, Stratford, CT, USA) for illumination

Table 1
Patient group with oral leukoplakia characteristics

Patient No.	Sex	Age	Site	Clinical diagnosis	Histology		
					Dysplasia grade 0–3	Hyperplasia grade 0–2	Hyperkeratosis grade 0–2
1	M	78	Floor	Homogenous	3	2	0
2	M	67	Lip	Non-homogenous/erosive	1	0	1
3	F	57	Floor	Non-homogenous/verrucous	0	1	2
4	F	81	Buccal fold	Homogenous	0	2	2
5	F	49	Floor	Homogenous	0	0	2
6	F	47	Pharynxbow	Homogenous	2	0	0
7	M	76	Lip	Homogenous	3	0	0
8	M	79	Lip	Non-homogenous/erosive	1	0	2
9/1st	F	62	Gingiva	Homogenous	0	1	2
9/2nd	F	62	Gingiva	Homogenous	0	1	2
10	M	30	Lip	Non-homogenous/verrucous	0	0	2
11	F	65	Tongue	Non-homogenous/verrucous	2	1	2
12	F	62	Buccal	Homogenous	3	2	2
13	M	79	Pharynxbow	Non-homogenous/erosive	2	2	1
14	F	48	Tongue	Homogenous	1	2	2
15	M	50	Trigonum	Non-homogenous/erosive	0	2	1
16	M	61	Tongue	Non-homogenous/verrucous	2	2	2
17	F	65	Floor	Non-homogenous/erosive	2	2	0
18	F	66	Floor	Homogenous	2	1	2
19	M	42	Floor	Homogenous	1	0	1
20	M	58	Lip	Non-homogenous/verrucous	0	2	2
21	M	60	Buccal	Non-homogenous/verrucous	0	2	2

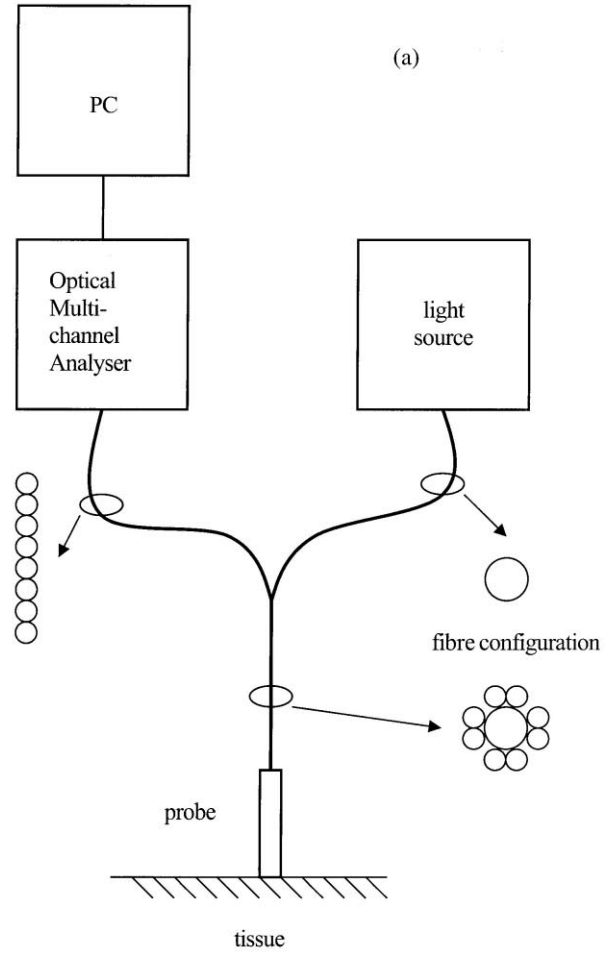

(b)

Fig. 1. (a) Experimental set-up for acquisition of tissue autofluorescence spectra. Low power illumination and fluorescence detection was performed with (b) an exchangeable measuring probe in contact with the oral mucosa.

and an optical multi-channel analyzer (OMA) (Instaspec-IV 77131 CCD-camera + Multispec 77400 spectrometer, Oriel Instruments Corporation) for spectroscopy. The light source and OMA were connected to the separate illumination and fluorescence detection arms of an Y-fibre. An exchangeable measuring probe, consisting of an imaging fibre bundle of 8 mm in diameter, was connected to the end of the third fibre arm where the illumination fibre and fluorescence detection fibre joined. Tissues were investigated under 420-nm excitation (bandwidth $\leqslant$15 nm Full Width Half Maximum) with a total output of 100 μW from the tip of the probe. Autofluorescence spectra were measured from 465 to 650 nm (475-nm long wavelength pass filter) with the OMA at an integration time of 1 s.

The measuring probes were disinfected in chlorhexidine gluconate and dried before use on a patient (Fig. 1b). Measurements were performed under a low ambient light level with the probe in contact with the oral mucosa. A measurement of a fluorescence spectrum at each site, as used in the analysis, was obtained by averaging three spectra measured sequentially at that site. First, at a normal site, contralateral to the lesion, a background spectrum was measured with the light source off followed by a normal fluorescence measurement (with the light source on). Next, fluorescence spectra were measured at the centre (one measurement), at the border (one or two measurements) and at the surrounding area of the lesion (one or two measurements). The background spectrum was subtracted from all fluorescence spectra.

The total number of spectra from the 21 patients amounted: centre lesion 22, border lesion 33, surrounding lesion area 33 and contralateral site 22; and the total number of spectra from the two investigators amounted: normal mucosa six and contralateral site six.

2.4. Training and evaluation of artificial neural networks

Spectral intensities were pre-scaled to values in the range 0–1, in order to suit the input of the neural network computer program. First, three consecutive data points were averaged to reduce the number of data points making up a spectrum. Second, the spectrum was divided by two times the corresponding contralateral spectrum. These procedures resulted in curves consisting of 175 normalised data points, spaced approximately 1 nm apart and centered around the value 0.5. Note that, ideally, the curve of normal tissue is a straight line with a y-value of 0.5.

For classification the pre-scaled autofluorescence spectra were entered into a neural network (type: fully connected layer-to-layer feedforward backpropagation network) [14]. The computer algorithm [15,16] modelled 4 layers of neurons (Fig. 2a). The first (input), second, third and fourth (output) layer consisted of 175, 100, $10\times n$ and n neurons, respectively, where n is the number of neurons in the output layer which could be either 2, 3, 4, 5 or 6. The 175 normalised data points of an autofluorescence curve are presented to the 175 neurons in the input layer. In a neuron (Fig. 2b), the inputs i_j (value between 0 and 1) are multiplied by numbers w_j (weights, value between -1 and 1), then summed and

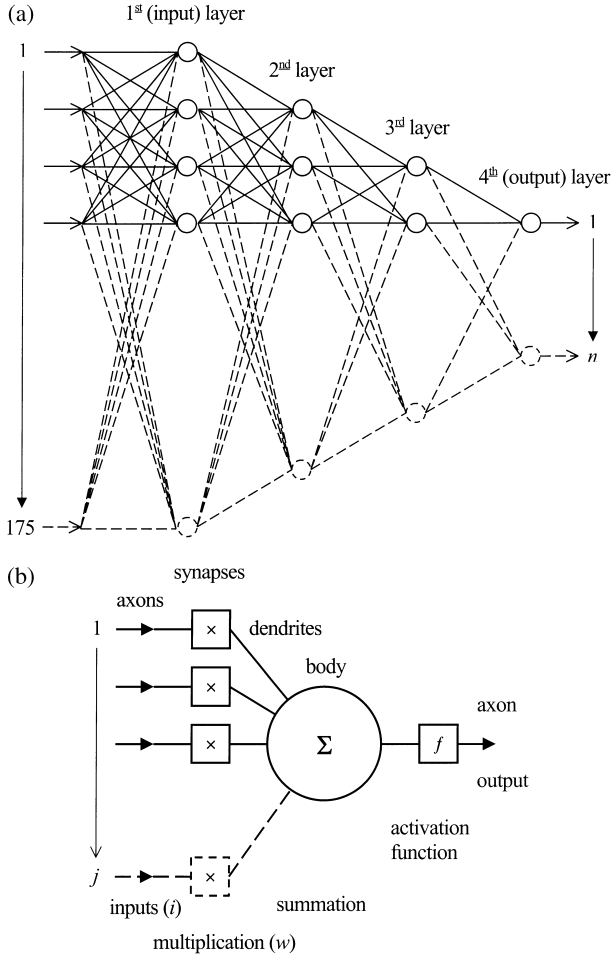

Fig. 2. (a) Model of the artificial neural network used for classification of autofluorescence spectra. Each node represents (b) a neuron, where the inputs (i_j) are multiplied by the weights (w_j), summed and inserted into an activation function (f).

the result is finally inserted in an activation function producing an output $f(x)$ (value between 0 and 1). Mathematically: $f(x) = (1 + e^{-ax})^{-1}$, where $x = \Sigma w_j i_j$ and a was 0.3, 0.4, 0.5 and 0.6 for the first, second, third and fourth layers, respectively. The total number of weights in a network amounted between 50,165 and 54,485 ($175\times175 + 175\times100 + 100\times10n + 10n\times n$, and n between 2 and 6).

Before any classification is possible one has to tell (train) a network what kind of output it should produce for a certain type of input curve. Training involves merely adaptation of all the weights in a network in such a way that for each individual training curve the output neurons produce their specified output. Several networks were trained for correlation of the pre-scaled spectra with either the clinical diagnosis or the histological classifications of dysplasia, hyperplasia, hyperkeratosis or grade thereof (Table 2). In order to make the utmost use of the few available curves, training and evaluation was performed cyclically using all 28 curves of the centre lesion and normal oral mucosa measurements instead of sub-dividing the only 28 curves in a training set and a test set. For each step in the cycle of 28 trainings and classifications, 27 of the 28 input/output combinations were presented for training and the 28th input curve was presented for blind classification. In other words, each of the 28 curves was once used for testing, while the other 27 curves were used for training.

Finally, the curves of the 33 border and 33 surrounding measurements of the lesions were assessed using neural networks with two and three output neurons (the best performing networks). In this case the neural networks were trained once using all 28 curves of the centre lesion and normal oral mucosa measurements.

3. Results

The acquired autofluorescence spectra of patients showed that the fluorescence intensity across the whole spectrum band varied for the different kinds of tissues (Fig. 3). The fluorescence of the centre of a lesion was usually lower than the fluorescence of the contralateral normal site. However, the fluorescence of the border of a lesion was often the lowest. Surrounding tissue of a lesion showed a fluorescence that was either higher or lower than the fluorescence of the contralateral normal site.

Also, the inter-patient variation of the fluorescence was considerable, i.e. the fluorescence intensity of, for instance, normal tissue could easily deviate 25% from patient to patient. This phenomenon was at least partly attributed to the individually varying optical properties. Pre-scaling of the raw fluorescence spectra (partly) neutralised this influence as well as minor variations in output power of the excitation light. Note that the resulting curves after pre-scaling only show the variation of the spectra with respect to the corresponding contralateral normal tissue spectra (Fig. 4) and that original fluorescence peaks and valleys are lost. Curves grouped according to the clinical diagnosis show that the fluorescence in the green region is decreasing with increasing degree of malignancy. Although this feature was obvious for the mean of several curves, it was rather difficult to (visually) classify an individual curve.

The results of the neural network classification of the blindly presented 22 curves of the centre lesion measurements and the six curves of normal oral mucosa are given in terms of sensitivity and specificity, where the clinical diagnosis and histological classification served as the gold standards (Table 3). The neural network (two output neurons) could distinguish abnormal tissue from normal tissue with a sensitivity of 86% and a specificity of 100%. Correct classification of either homogenous, non-homogenous or normal tissue (three output neurons) was performed amply above random percentages for the sensitivity and specificity (73 and 82%, 64

Table 2
Neural network input/output for training and evaluation

Input curve	No. of curves	No. of output neurons	Presented/desired output at neuron No.					
			1	2	3	4	5	6
Normal	6	2	1	0	NA[a]	NA	NA	NA
Abnormal	22		0	1	NA	NA	NA	NA
Normal	6	3	1	0	0	NA	NA	NA
Homogenous	11		0	1	0	NA	NA	NA
Non-homogenous	11		0	0	1	NA	NA	NA
Normal	6	4	1	0	0	0	NA	NA
Homogenous	11		0	1	0	0	NA	NA
Verrucous	6		0	0	1	0	NA	NA
Erosive	5		0	0	0	1	NA	NA
Normal	6	4[b]	1	0	0	0	NA	NA
Dysplasia	13		0	1	–	–	NA	NA
Hyperplasia	15		0	–	1	–	NA	NA
Hyperkeratosis	18		0	–	–	1	NA	NA
Normal	6	4	1	0	0	0	NA	NA
Abnormal/no hyperplasia	7		0	1	0	0	NA	NA
Hyperplasia grade 1	5		0	0	1	0	NA	NA
Hyperplasia grade 2	10		0	0	0	1	NA	NA
Normal	6	4	1	0	0	0	NA	NA
Abnormal/no hyperkeratosis	4		0	1	0	0	NA	NA
Hyperkeratosis grade 1	4		0	0	1	0	NA	NA
Hyperkeratosis grade 2	14		0	0	0	1	NA	NA
Normal	6	5	1	0	0	0	0	NA
Abnormal/no dysplasia	9		0	1	0	0	0	NA
Dysplasia grade 1	4		0	0	1	0	0	NA
Dysplasia grade 2	6		0	0	0	1	0	NA
Dysplasia grade 3	3		0	0	0	0	1	NA
Normal	6	6[b]	1	0	0	0	0	0
Homogenous	11		0	1	0	–	–	–
Non-homogenous	11		0	0	1	–	–	–
Dysplasia	13		0	–	–	1	–	–
Hyperplasia	15		0	–	–	–	1	–
Hyperkeratosis	18		0	–	–	–	–	1

[a] Not applicable.
[b] Adds up to more than 28 input curves as lesions can have multiple aberrations (–, can be either 0 or 1 for individual curves).

and 94%, 100 and 86%, respectively). Further subdivision of the clinical diagnosis (four output neurons) yielded a 0% sensitivity for verrucous and erosive tissue. Classification by the neural network of tissue dysplasia, hyperplasia, hyperkeratosis, the grade thereof; or in combination with the clinical diagnosis (4–6 output neurons) was not feasible.

The results of the neural network classification of the blindly presented curves of the 33 border and 33 surrounding measurements of the lesions are given in Table 4. Most of these curves were classified as abnormal. This suggests that less visible tissue dysplasia can also be classified. However, this interpretation is somewhat hampered as no biopsies were taken at those measurement sites and thus a definite diagnosis was not available.

4. Discussion

In this study clinically evident leukoplakias were tested with autofluorescence spectroscopy. Especially the difference between the border of the lesion and the surrounding tissue is an interesting result and may be useful for the detection of margins or even not clinically visible lesions. This pilot study shows that neural networks perform fairly well in classifying autofluorescence spectra of visible leukoplakia as abnormal, homogenous or non-homogenous. Neural networks are therefore very helpful for the management of the enormous amount of data points that are produced during autofluorescence spectroscopy. A neural network may not be the best way to analyse autofluorescence spectra for the diagnostic problem discussed in this paper. We

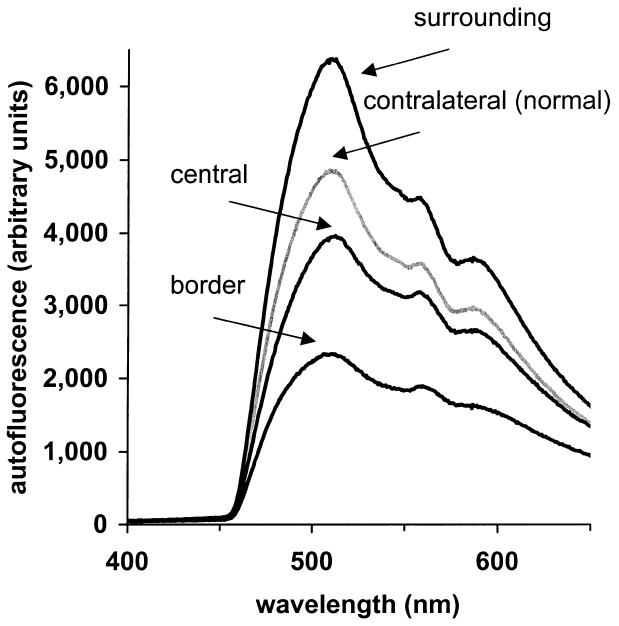

Fig. 3. Example of oral mucosa fluorescence (420 nm excitation) of a patient bearing leukoplakia.

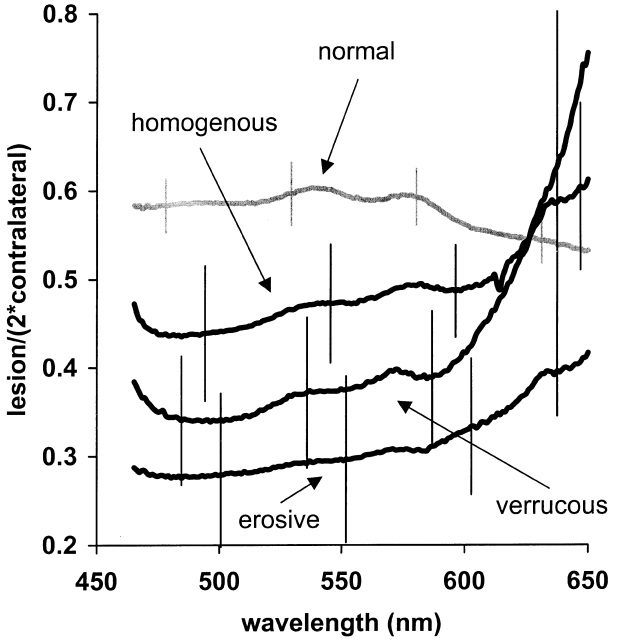

Fig. 4. Example of mean neural network input curves grouped according to the clinical diagnosis. Individual curves are used for training or evaluation of the neural network. Error bars indicate the standard error of the mean.

Table 3
Neural network performance compared to the gold standards of clinical diagnosis and histological classification.[a] For calculation of the sensitivity and specificity the spectra were allocated to the two groups X and not-X, where X is the classification.

No. of output neurons	Classification	Score	Sensitivity (%)	Specificity (%)
2	Abnormal	19/22	86	100
	Normal	6/6	100	86
3	Homogenous	8/11	73	82
	Non-homogenous	7/11	64	94
	Normal	6/6	100	86
4	Homogenous	6/11	55	82
	Verrucous	0/6	0	77
	Erosive	0/5	0	83
	Normal	6/6	100	82
4[b]	Dysplasia	4/13	31	67
	Hyperplasia	10/15	67	69
	Hyperkeratosis	10/18	56	60
	Normal	5/6	83	86
4	Abnormal/no hyperplasia	2/7	29	90
	Hyperplasia grade 1	0/5	0	83
	Hyperplasia grade 2	4/10	40	67
	Normal	6/6	100	82
4	Abnormal/no hyperkeratosis	0/4	0	79
	Hyperkeratosis grade 1	0/4	0	92
	Hyperkeratosis grade 2	5/14	36	57
	Normal	6/6	100	82
5	Abnormal/no dysplasia	1/9	11	58
	Dysplasia grade 1	0/4	0	96
	Dysplasia grade 2	0/6	0	73
	Dysplasia grade 3	2/3	67	92
	Normal	4/6	67	82
6[c]	Homogenous	5/11	45	71
	Non-homogenous	5/11	45	76
	Dysplasia	6/13	46	67
	Hyperplasia	9/15	60	77
	Hyperkeratosis	10/18	56	50
	Normal	6/6	100	91

[a] Networks were cyclically trained and evaluated using the 28 spectra measured at the centre of lesions and at normal oral mucosa; 28 times, 27 curves were presented for training and the 28th curve was blindly classified.

[b] Perfect classification of lesion spectra 2/22.

[c] Perfect classification of lesion spectra 0/22.

have chosen the neural network approach because it seemed practical and the use of this technique for autofluorescence diagnostics had not yet been reported.

A tissue characterising system, combining autofluorescence spectroscopy and neural networks, would be a clinically useful tool. To the best of our knowledge, the only publication reporting about classification of autofluorescence spectra (in the visible part of the spectrum) using neural networks is by Gindi et al. [13]. They investigated the possibility of distinguishing atherosclerotic plaque from normal tissue. The technique could be deployed in oral and maxillofacial surgery (1) to guide conventional biopsy, which may reduce the number of biopsies taken, or (2) to demarcate accurately

Table 4
Neural network performance[a]

Input	No. of output neurons	Classification	Score
Border spectra	2	Abnormal	28/33
		Normal	5/33
Surrounding spectra	2	Abnormal	31/33
		Normal	2/33
Border spectra of homogenous lesions	3	Homogenous	9/17
		Non-homogenous	7/17
		Normal	1/17
Surrounding spectra of homogenous lesions	3	Homogenous	10/17
		Non-homogenous	6/17
		Normal	1/17
Border spectra of non-homogenous lesions	3	Homogenous	9/16
		Non-homogenous	6/16
		Normal	1/16
Surrounding spectra of non-homogenous lesions	3	Homogenous	8/16
		Non-homogenous	6/16
		Normal	2/16

[a] Networks were trained one time using all 28 spectra measured at the centre of lesions and at normal oral mucosa; border and surrounding spectra were blindly classified.

the diseased tissue area for CO_2-laser evaporation, which may spare surrounding normal tissue or even prevent exclusion of invisible leukoplakia. Another indication may be (3) to plan the extent of a resection of a SCC. The ideal clinical system would be a scanning or even better an imaging system, where an autofluorescence spectrum is taken from each image pixel. The spectra should be analysed in real-time and detected tissue abnormalities should then be reported either visually or auditively.

In this study, the results were obtained using relatively few training examples for the neural networks. As a rule of thumb, the number of independent facts for training must be 10 times the number of adjustable weights in the neural network. We had 28 spectra at our disposal in this study, far from the required 500,000 for the networks having over 50,000 weights. This may suggest that the use of more training spectra can further improve the sensitivity and specificity for several other tissue characteristics as dysplasia, hyperplasia and hyperkeratosis. Another cause of classification errors may be the pre-scaling procedure, where lesion spectra were divided by contralateral spectra. After all, in patients, the contralateral site is not necessarily normal tissue (possibility of condemned mucosa). The low correlation of the autofluorescence with dysplasia may also be caused by the hyperkeratosis that shields the underlying tissue from the excitation light and the measuring probe from the tissue fluorescence. Therefore, dysplastic lesions without hyperkeratosis may be suitable for histological grading with the neural network method.

The choice of 420-nm excitation wavelength in this study was guided by previous investigations with excitation wavelengths in the range of 400–450 nm [3,4]. At this wavelength several endogenous tissue fluorophores can be excited, viz. porphyrins, lipo-pigments and flavins, which have a fluorescence emission in the range of 450–650 nm [2]. The peak fluorescence of leukoplakia in the green region centered at 515 nm is decreasing with increasing degree of malignancy, as compared to normal or contralateral mucosa. This is a known general feature of the autofluorescence and was reported previously for the upper aerodigestive tract by Dhingra et al. [3], Harries et al. [4] and Roy et al. [5]. Also, the often lower fluorescence of the border of a lesion as compared to the fluorescence of the centre of a lesion was observed previously in the oral cavity by Fryen et al. [7]. The basis for these extreme autofluorescence spectra might possibly also be found in an inflammatory reaction of the tissue surrounding a lesion. As a consequence in this case, as inflammation was not a possible output of the neural networks, the classification of these sites as dysplastic would be erroneous.

To conclude, our in vivo study on human oral mucosa shows that neural networks can provide a very good discrimination between autofluorescence spectra of leukoplakia and normal tissue. One has to keep in mind that this pilot study was performed on histologically proven visible lesions and the technique's usefulness for early pre-malignant lesions has yet to be established. In the near future a prospective study will be conducted, where patients will be followed for several years. This will yield a much larger database of oral autofluorescence spectra at multiple excitation wavelengths with which we might be able to answer some of the questions raised.

Acknowledgements

We are grateful to the patients for their valuable contribution and we thank the fellow workers Riëtte, Lars, Hanneke and Ronald for undergoing the many trial measurements. This study was partially supported by the Dutch Cancer Society (''Nederlandse Kanker Bestrijding''), grant DDHK 95-1062.

References

[1] Van der Waal I, Schepman KP, Van der Meij EH, Smeele LE. Oral leukoplakia: a clinicopathological review. Oral Oncology 1997;33:291–301.
[2] Wagnières GA, Star WM, Wilson BC. In vivo fluorescence spectroscopy and imaging for oncological applications. Photochemistry and Photobiology 1998;68:603–32.
[3] Dhingra JK, Perrault DF, McMillan K, Rebeiz EE, Kabani S, Manoharan R, Itzkan I, Feld MS, Shapshay SM. Early diagnosis of upper aerodigestive tract cancer by autofluorescence. Archives of Otolaryngology–Head and Neck Surgery 1996;122:1181–6.

[4] Harries ML, Lam S, Macaulay C, Qu J, Palcic B. Diagnostic imaging of the larynx: autofluorescence of laryngeal tumours using the helium–cadmium laser. Journal of Laryngology and Otology 1995;109:108–10.
[5] Roy K, Bottrill ID, Ingrams DR, Pankratov MM, Rebeiz EE, Woo P, Kabani S, Shapshay SM, Manoharan R, Itzkan I, Feld MS. Diagnostic fluorescence spectroscopy of oral mucosa. In: Anderson RR, editor. SPIE proceedings 2395, Lasers in surgery: advanced characterization, therapeutics, and systems V. Bellingham. Washington: SPIE, 1995. p. 135–42.
[6] Wang C-Y, Chiang HK, Chen C-T, Chiang C-P, Kuo Y-S, Chow S-N. Diagnosis of oral cancer by light-induced autofluorescence spectroscopy using double excitation wavelengths. Oral Oncology 1999;35:144–50.
[7] Fryen A, Glanz H, Lohmann W, Dreyer T, Bohle RM. Significance of autofluorescence for the optical demarcation of field cancerisation in the upper aerodigestive tract. Acta Otolaryngologica (Stockholm) 1997;117:316–9.
[8] Mizuno-Matsumoto Y, Inouye T, Tamura S. Occurrences of electroencephalographic (EEG) patterns that resemble epileptiform discharges in background EEG in epileptic patients. International Journal of Neuroscience 1997;91:69–84.
[9] Zatari D, Botros N, Dunn F. In vivo liver differentation by ultrasound using an artificial neural network. Journal of the Acoustical Society of America 1994;96:376–81.
[10] Lisboa PJ, Kirby SP, Vellido A, Lee YY, El-Deredy W. Assessment of statistical and neural networks methods in NMR spectral classification and metabolite selection. NMR in Biomedicine 1998;11:225–34.
[11] Benaron DA, Cheong W-F, Duckworth JL, Noles K, Nezhat C, Seidman D, Hintz SR, Levinson CJ, Murphy AL, Price JW, Liu FWH, Stevenson DK, Kermit EL. Automated classification of tissue by type using real-time spectroscopy. In: Sevick-Muraca EM, Izatt JA, Ediger MN, editors. OSA trends in optics and photonics vol. 22, Biomedical optical spectroscopy and diagnostics/therapeutic laser applications. Washington (DC): Optical Society of America, 1998. p. 30–4.
[12] Pizzi N, Choo LP, Mansfield J, Jackson M, Halliday WC, Mantsch HH, Somorjai RL. Neural network classification of infrared spectra of control and Alzheimer's diseased tissue. Artificial Intelligence in Medicine 1995;7:67–79.
[13] Gindi GR, Darken CJ, O'Brien KM, Stetz ML, Deckelbaum LI. Neural network and conventional classifiers for fluorescence-guided laser angioplasty. IEEE Transactions on Biomedical Engineering 1991;38:246–52.
[14] Haykin S. Neural networks. New York: Macmillan College Publishing Company, 1994.
[15] Rao VB, Rao HV. C++ neural networks and fuzzy logic. New York: MIS Press, 1995.
[16] Page GF, Gomm JB, Williams D, editors. Application of neural networks to modelling and control. London: Chapman & Hall, 1993.